Annals of Nuclear Medicine (2021) 35:649–661
https://doi.org/10.1007/s12149-020-01569-1

ORIGINAL ARTICLE

Comparison of the detecting capability between ^{123}I-mIBG and post-therapeutic ^{131}I-mIBG scintigraphy for curie scoring in patients with neuroblastoma after chemotherapy

Zhong-Ling Qiu[1] · Shintaro Saito[2] · Daiki Kayano[2] · Hiroshi Wakabayashi[2] · Seigo Kinuya[2]

Received: 13 October 2020 / Accepted: 11 December 2020 / Published online: 17 April 2021

Abstract

Objective To evaluate the detecting capability between planar imaging (PI) and PI combined with single-photon emission computed tomography/computed tomography (PICWS), including ^{123}I- and ^{131}I-labeled metaiodobenzylguanidine (mIBG) and to compare the detecting capability between ^{123}I-mIBG and post-therapeutic ^{131}I-mIBG scintigraphy including PI and PICWS for Curie scoring in patients with neuroblastoma.

Methods Sixty-two patients with 66 pairs of complete images with neuroblastoma were enrolled in this retrospective study.

Results Comparing the Curie scoring between ^{123}I-mIBG PI and PICWS and between post-therapeutic ^{131}I-mIBG PI and PICWS, findings were concordantly negative in 28.79% and 18.18% of studies, concordantly positive in 66.67% and 74.24% of studies, and discordant in 4.54% and 7.58% of studies, respectively. PICWS was superior to PI including ^{123}I- and ^{131}I-mIBG in the evaluation of Curie scoring for neuroblastoma patients (both $P < 0.001$). Comparing the Curie scores between ^{123}I- and post-therapeutic ^{131}I-mIBG PI and between ^{123}I- and post-therapeutic ^{131}I-mIBG PICWS, concordantly negative imaging was visualized in 22.73% and 19.70% of studies, concordantly positive imaging in 66.67% and 69.70% of studies, and discordant imaging in 10.60% and 10.60% of studies, respectively. Post-therapeutic ^{131}I-mIBG was significantly better than that of ^{123}I-mIBG scintigraphy including PI and PICWS in detecting the Curie scoring for neuroblastoma patients (both $P < 0.001$).

Conclusion The present study demonstrates that ^{131}I- or ^{123}I-mIBG PICWS are more helpful in the evaluation of Curie scores than that of conventional PI and that post-therapeutic ^{131}I-mIBG is superior to ^{123}I-mIBG scintigraphy for the detecting capability of Curie scoring in patients with neuroblastoma.

Keywords ^{123}I-mIBG scintigraphy · ^{131}I-mIBG scintigraphy · Curie scoring · Neuroblastoma · Single-photon emission computed tomography/computed tomography

Introduction

Originating from the neural crest with an incidence ranging from 2.7 to 12%, neuroblastoma is the most common extracranial solid malignant tumor in children, [1, 2]. Approximately, 50% of the cases arise in the adrenal gland, but neuroblastomas can occur in any part of the body along the sympathetic nervous system, including the abdomen, chest, neck, and pelvis [1]. Approximately, 70% of patients with neuroblastomas experience metastatic diseases, which are usually seen in bones, lymph nodes, liver, and lungs in the early stages of the disease [3].

As an analog of neurotransmitter norepinephrine, metaiodobenzylguanidine (mIBG) can be absorbed and aggregated in neural crest tumors such as pheochromocytoma,

Zhong-Ling Qiu and Shintaro Saito Joint first authors contributed equally to this work.

✉ Daiki Kayano
kayano@staff.kanazawa-u.ac.jp

[1] Department of Nuclear Medicine, Shanghai Jiao Tong University Affiliated Sixth People's Hospital, 600 Yishan Road, Shanghai 200233, China

[2] Department of Nuclear Medicine, Kanazawa University Hospital, 13-1 Takara-machi, Kanazawa, Ishikawa 920-8641, Japan

paraganglioma, and neuroblastoma [4]. ^{131}I- and ^{123}I-mIBG scintigraphy are indispensable for the management of patients with neuroblastomas and have been widely used to detect metastatic and recurrent lesions in patients with neuroblastoma for more than three decades [4]. ^{123}I- and ^{131}I-mIBG planar imaging (PI) has been shown to have higher sensitivity of 88–93% and specificity of 83–92% for the detection of metastatic and recurrent lesions in neuroblastoma. Therefore, it has been implemented as a mandatory test in the International Neuroblastoma Risk Group Staging System, an imaging-defined staging and risk assessment system for neuroblastomas [5, 6]. In terms of the detection capability, ^{123}I-mIBG is superior to diagnostic ^{131}I-mIBG PI in finding metastatic and recurrent lesions of neuroblastoma, pheochromocytoma, and paraganglioma because of its more favorable gamma radiation energy [7, 8]; whereas, ^{123}I-mIBG is inferior to post-therapy ^{131}I-mIBG PI for its detection [9, 10]. Although ^{123}I- and ^{131}I-mIBG PI show higher sensitivity and specificity for their detection capability, the lack of anatomical landmarks is the main drawback, causing difficulty in accurately locating the focus of ^{123}I- or ^{131}I-mIBG uptake. An integrated single-photon emission computed tomography (SPECT)/computed tomography (CT) fusion system enables a direct correlation between functional and anatomical information, leading to better location and definition of the lesions in various neuroendocrine tumors. SPECT/CT has been widely used in the past decade [11] and has been found to be more valuable than PI in patients with neuroblastoma for correct characterization of the ambiguous ^{123}I- or ^{131}I-mIBG uptake seen in PI [9].

Curie scoring, a semi-quantitative scoring system, has been developed to predict the treatment response and prognosis of mIBG-avid disease for more than two decades, because of its good reproducibility and reliability with intraobserver and interobserver consistency [12]. Because of its higher sensitivity and specificity for diagnosing, staging, and monitoring response to therapy in neuroblastoma, ^{123}I- and ^{131}I-mIBG PI have been used to score using the Curie methods [12, 13]. However, to our best knowledge, regarding metastases and recurrence of neuroblastoma, few studies have directly compared ^{123}I- and ^{131}I-mIBG scintigraphy in terms of their detecting capability in estimating Curie scoring.

The present study aimed to compare the detecting capability between ^{123}I-mIBG and post-therapy ^{131}I-mIBG scintigraphy including ^{131}I- and ^{123}I-mIBG PI, and ^{131}I- and ^{123}I-mIBG PI combined with SPECT/CT (PICWS) and to evaluate the incremental value of ^{123}I-mIBG and post-therapy ^{131}I-mIBG PICWS compared with that of conventional PI for Curie scoring in patients with neuroblastoma.

Materials and methods

Patients

The medical records and images of 63 patients with neuroblastomas between January 2009 and December 2019 were analyzed retrospectively in the present study. Patients visited the Department of Nuclear Medicine of Kanazawa University Hospital, which is a major referral site for ^{131}I-mIBG treatment in Japan. The present study was approved by the Institutional Review Board of Kanazawa University Hospital. The inclusion criteria for patients with neuroblastoma were as follows: (1) all patients underwent at least one cycle of ^{131}I-mIBG treatment, (2) all patients were subjected to ^{123}I-mIBG PICWS within 2 weeks prior to ^{131}I-mIBG treatment, (3) all patients experienced ^{131}I-mIBG PICWS 2 to 5 days after ^{131}I-mIBG injection, and (4) all patients had more than one mIBG-avid lesion identified by ^{123}I-mIBG scintigraphy at the initial diagnosis before starting any treatment. Of the patients, one with poor ^{123}I-mIBG imaging quality was excluded. A total of 62 patients were finally enrolled in the present study. Written informed consent was obtained from all patients or their guardians before starting ^{131}I-mIBG treatment.

^{131}I-mIBG treatment

In our hospital, ^{131}I-mIBG treatment was conducted according to the guidelines of the European Association of Nuclear Medicine [14]. ^{131}I-mIBG was given to patients who were believed to receive a therapeutic benefit according to the results of ^{123}I-mIBG scintigraphy conducted 2 weeks prior to ^{131}I-mIBG treatment. To protect thyroid tissue from being destroyed by ^{131}I, patients were asked to take the 100–200 mg of potassium iodide orally beginning 1 day prior to ^{131}I-mIBG administration until 10 days post-therapy. The ^{131}I-mIBG was injected intravenously for at least 1 h, with a regular dose ranging from 148 to 666 MBq/kg, using a lead-shielded injection pump and through a peripheral fixed intravenous catheter in a standard radiation isolation room. Patients received the maximum dose of 24,420 MBq (660 mCi) owing to legal regulations.

^{131}I-mIBG planar and ^{131}I-mIBG SPECT/CT scintigraphy protocol

^{131}I-mIBG whole-body PI was obtained, including anterior and posterior projections, using a dual-headed gamma camera system with SPECT/CT (SymbiaT6; Siemens Medical Solutions [January 2009–December 2019]; or Discovery NM/CT 670 Q Suite Pro; GE Healthcare [December

2015–December 2019]) 2–5 days after ^{131}I-mIBG treatment. The camera system was equipped with a high energy parallel hole collimator (energy peak set at 364 keV ± 20%; 256 × 1024 matrix), using the continuous acquisition mode with a scanning speed of 15 cm/min. When any suspected of abnormal ^{131}I-mIBG concentration was found in the whole-body PI, SPECT/CT was conducted immediately after PI was completed. The SPECT portion was acquired using sixty 20-s projections over 360° with a 128 × 128 matrix. SPECT data were reconstructed using a three-dimensional iterative algorithm with ordered-subset expectation maximization. Immediately after SPECT acquisition, a CT image was acquired, followed by a spiral CT acquisition. The following CT acquisition parameters were used: tube current, 40 mA; collimation, 2 × 2.5 mm; and pitch, 2. CT data reconstruction was used for a 3-mm slice thickness with 2-mm slice increments. SPECT/CT data were analyzed on an e-soft workstation, displaying sagittal, transaxial, and coronal slices of SPECT, CT, and fused SPECT/CT imaging.

^{123}I-mIBG planar and ^{123}I-mIBG-SPECT/CT scintigraphy protocol

^{123}I-mIBG planar combined with SPECT/CT imaging was acquired in the same way as ^{131}I-mIBG planar combined with SPECT/CT scintigraphy, except for the use of a low-energy collimator with a photo peak of 159 keV. ^{123}I-mIBG scintigraphy was conducted after intravenous injection of 111 or 222 MBq of ^{123}I-mIBG using a dual-head gamma camera equipped with a low–medium-energy general-purpose collimator. Whole-body PI was obtained at 6 and 24 h after ^{123}I-mIBG administration. PI was conducted 6 h after tracer injection in all patients, and ^{123}I-mIBG SPECT/CT imaging was obtained based on the previously described ^{131}I-SPECT/CT imaging acquisition pattern. In our study, the 111 or 222 MBq of ^{123}I-mIBG dose was used for ^{123}I scintigraphy, because until May 2011, only 111 MBq of ^{123}I-mIBG was allowed for patients according to the Japanese regulations, which is relatively lower than the standard dose of ^{123}I-mIBG in Western countries. After May 2011, 222 MBq was allowed for the patients in Japan, which was similar to the standard dose of ^{123}I-mIBG in Western countries.

Curie scoring

For every image, ^{123}I- and ^{131}I-mIBG scintigraphy were scored using the Curie methods [12]. According to the Curie semi-quantitative scoring method, scores were evaluated as follows: the skeleton was divided into nine body segments, with a tenth section added for soft tissue lesions. The areas of the skeleton included (1) the head and face; (2) the neck and back vertebral column; (3) the ribs, sternum, and scapula; (4) the lumbar and sacral column; (5) the pelvis; (6) the arms; (7) the forearms and hands; (8) the thighs; and (9) the legs and feet. The mIBG avidity of the nine body segments was scored on a scale ranging from 0 to 3, depending on the extent of the disease, with 0 indicating no site per segment, 1 indicating one site per segment, 2 indicating more than one site per segment, and 3 indicating diffuse involvement (> 50% of the segment area). Soft tissue lesions were scored as follows: 0 (no mIBG-avid lesion), 1 (1 mIBG-avid lesion), 2 (more than one mIBG-avid lesion), and 3 (mIBG-avid lesions occupying > 50% of the chest or abdomen). The overall absolute scores were obtained by adding the corresponding scores for each region (up to 30 points). The total Curie scores of each image were defined as the scores of all subjects added up.

Image interpretation

All ^{123}I-, ^{131}I-mIBG PI and PICWS were scored according to the number of all mIBG-avid lesions by an experienced nuclear medicine physician with 12 years of experience in reading ^{123}I- and ^{131}I-mIBG imaging, who was blinded to the results for the other imaging modalities. When a lesion in the image was interpreted as indeterminate, the score was determined in consultation with two other experienced nuclear medicine physicians with 9 and 13 years of experience, respectively, who reviewed the ^{123}I and ^{131}I-mIBG images. Diffuse mIBG uptake at the nasal cavity, salivary glands, thyroid, myocardium, liver, intestinal tract, and bladder were considered as physiological uptake. SPECT/CT images were evaluated for Curie scoring based on the location of the lesions detected in PI or identifying new lesions. In the absence of mIBG-avid lesions in the SPECT images, suspected metastatic findings in CT alone were not considered as a new lesion. Consensus was also acquired with another experienced nuclear medicine physician in the same way as the PI if the interpretation for score was uncertain. Score was considered negative if there was no abnormal ^{131}I- or ^{123}I-mIBG accumulation apart from physiological uptake. Scores were considered positive if there was at least one lesion with abnormal ^{131}I-mIBG uptake.

Statistical analysis

SPSS 17.0 (SPSS Inc., Chicago, IL) was used for statistical analysis. Continuous data were shown as mean ± standard deviation (SD) with range and median, and categorical data were displayed as an absolute number with percentage. Comparing the diagnostic value between ^{123}I-mIBG and post-therapeutic ^{131}I-mIBG scintigraphy and the incremental value of ^{123}I-mIBG and post-therapeutic ^{131}I-mIBG PICWS over PI for Curie scoring was estimated using the Wilcoxon

signed-rank test. A *P*-value of less than 0.05 was considered a statistically significant difference.

Results

Patient characteristics

The clinical and pathological characteristics of the 62 patients with neuroblastoma are summarized in Table 1. The mean age at the time of the initial diagnosis of neuroblastoma was 5.32 ± 4.08 years (median, 4 years; range, 0–21 years). Of the 62 patients, 35 (56.45%) were male and 27 (43.55%) were female, resulting in a male: female ratio of 1.30:1.00. All patients received at least five cycles of chemotherapy prior to ^{131}I-mIBG treatment. Among them, 55 (88.71%) patients had one cycle of ^{131}I-mIBG treatment, five had two cycles, and two had three cycles. Theoretically, there should be 71 pairs of ^{123}I- and post-therapeutic ^{131}I-mIBG PI combined with SPECT/CT conducted within 2 weeks in these 62 patients. However, only 66 pairs of complete imaging were obtained and reviewed, including 58 cases with a pair of images and four patients with two pairs of images.

Evaluation of Curie scoring and its distribution

For ^{123}I-mIBG PI, ^{123}I-mIBG PICWS, ^{131}I-mIBG PI, and ^{131}I-mIBG PICWS, the total Curie scores were 356, 411, 469, and 508, respectively, in 62 patients with 66 sets of matched imaging (Table 2; Fig. 1a). In ^{123}I-mIBG PI, 44 (66.67%) of the cases showed positive results with a median Curie score of 5 (range, 1–23; mean ± SD, 8.09 ± 6.89) and the remainder had negative results. In ^{123}I-mIBG PICWS,

Table 1 Patients' characteristics

Characteristics	*N* (%)
Age at initial diagnosis (years) (mean ± SD, median, range)	5.32 ± 4.08, 4, 0–21
Age at initial ^{131}I-mIBG therapy (years) (mean ± SD, median, range)	9.01 ± 4.57, 8, 1–22
Sex	
Male	35 (56.45%)
Female	27 (43.55%)
INSS at initial diagnosis	
3	7 (11.29%)
4	54 (87.10%)
Unknown	1 (1.61%)
Primary site	
Adrenal	40 (664.52%)
Mediastinum	6 (9.68%)
Intra-abdominal beside adrenal	11 (17.74%)
Pelvis	2 (3.22%)
Paraspinal sympathetic ganglion	2 (3.22%)
Cranial base	1 (1.61%)
Initial surgery	
Complete tumor removal	43 (69.35%)
Partial tumor removal	11 (17.74%)
No surgery	8 (12.91%)
Histology	
Neuroblastoma	55 (88.71%)
Ganglioneuroma	7 (11.29%)
^{131}I-mIBG dose (Mean ± SD, Median, Range)	417.90 ± 215.42, 350, 90–1360
Number of courses for ^{131}I-mIBG therapy	
1	55 (88.71%)
2	5 (8.06%)
3	2 (3.23%)
Time from closest chemotherapy to ^{131}I-mIBG therapy (months)	6.24 ± 8.48, 4, 1–60
Time from initial diagnosis to ^{131}I-mIBG therapy (months)	42.32 ± 33.03, 35.00,0–177

SD Standard deviation, *INSS* International Neuroblastoma Risk Group Staging System, *mIBG* metaiodobenzylguanidine

Table 2 Distribution of the Curie scores in 66 pairs of ^{123}I-and post-therapy ^{131}I-mIBG scinitgraphies conducted in 62 patients

Location	^{123}I-mIBG PI		^{123}I-mIBG PICWS		^{131}I-mIBG PI		^{131}I-mIBG PICWS	
	Scores	*N* (%)	Scores	*N* (%)	Scores	*N* (%)	Scores	*N* (%)
1	45	28 (42.42%)	45	26 (39.39%)	59	32 (48.48%)	60	32 (48.48%)
2	42	20 (30.30%)	47	22 (33.33%)	57	26 (39.39%)	63	28 (42.42%)
3	46	28 (42.42%)	52	29 (43.94%)	48	27 (40.91%)	55	31 (46.97%)
4	47	21 (31.81%)	59	30 (45.45%)	66	29 (43.94%)	69	31 (46.97%)
5	52	27 (40.90%)	57	28 (42.42%)	68	34 (51.52%)	69	32 (48.48%)
6	27	14 (21.21%)	33	16 (24.24%)	43	22 (33.33%)	44	22 (33.33%)
7	7	4 (6.06%)	7	4 (6.06%)	12	7 (10.61%)	12	7 (10.61%)
8	49	26 (39.39%)	50	26 (39.39%)	64	27 (40.91%)	66	30 (45.45%)
9	31	18 (27.27%)	31	18 (27.27%)	39	22 (33.33%)	38	22 (33.33%)
10	10	5 (7.58%)	30	22 (33.33%)	13	8 (12.12%)	32	25 (37.88%)
Total	356	44 (66.67%)	411	47 (71.21%)	469	51(77.27%)	508	52 (78.79%)

Locations: **1,** the head and the face; **2,** the neck and back vertebral column; **3,** the ribs, the sternum and scapula; **4,** the lumbar and sacral column; **5,** the pelvis; **6,** the arms; **7,** the fore- arms and the hands; **8**, the thighs; **9,** the legs and the feet; **10,** soft tissues

mIBG metaiodobenzylguanidine, *PI* planar imaging, *PICWS* planar imaging combined with single-photon emission computed tomography/computed tomography

47 (71.21%) of the cases had positive results and 19 had negative results. The median Curie score in the positive group was 7 (range, 1–24; mean ± SD, 8.74 ± 6.88). In ^{131}I-mIBG PI, 51 (77.27%) of the cases were classified as positive results, with a median Curie score of 7 (range, 1–24; mean ± SD, 9.20 ± 7.65). The 15 remaining cases were considered to have negative results. In ^{131}I-mIBG PICWS, 52 (78.79%) of the images were interpreted as positive results, with a median Curie score of 8.5 (range, 1–24; mean ± SD, 9.77 ± 7.60), and the remaining 14 were considered as negative results (Fig. 1b). The scores for each segment of the body of 66 pairs of matched scintigraphy in 62 patients are presented in Table 2.

^{123}I-mIBG PICWS versus ^{123}I-mIBG PI for Curie scoring

In a comparison of all 66 pairs of ^{123}I-mIBG PI and ^{123}I-mIBG PICWS, summarized in Tables 2 and 3 and Fig. 1c, we found that ^{123}I-mIBG PICWS could detect 55 more scores than ^{123}I-mIBG PI according to the Curie scoring criteria (411 vs. 356) and that ^{123}I-mIBG PICWS changed the scores of 50% of the studies compared with ^{123}I-mIBG PI. Considering each body segment, the advantages of ^{123}I-mIBG PICWS compared with PI in evaluating Curie scoring focused mainly on soft tissue lesions [10]; the lumbar and sacral column [4]; and the ribs, sternum, and scapula [3], with additional scores in PICWS for 20 (30 vs. 10), 12 (59 vs. 47), and 6 (52 vs. 46), respectively. Globally, ^{123}I-mIBG PI and PICWS findings were concordantly negative in 28.79% of images in evaluating the Curie scoring, findings were concordantly positive in 66.67% of images, and findings were discordant in 4.54% of images. In concordant positive studies, ^{123}I-mIBG PICWS had the same scores (125 vs. 125) as ^{123}I-mIBG PI in 14 (21.21%) studies, ^{123}I-mIBG PICWS had higher scores than those of ^{123}I-mIBG PI in 29 (43.94%) studies with the scores of 278 versus 226 (Fig. 2), and ^{123}I-mIBG PICWS had lower scores than those of ^{123}I-mIBG PI in one study with the scores of 4 versus 5. In disconcordant imaging, three (4.54%) images with a score of 4 were noted in the ^{123}I-mIBG SPECT/CT but could not be found in the ^{123}I-mIBG PI (Table 3). The 66 pairs of ^{123}I-mIBG PI and ^{123}I-mIBG PICWS suggested the superiority of the latter modality in detecting Curie scoring using the Wilcoxon signed-rank test ($Z = -4.83$; $P < 0.001$).

^{131}I-mIBG PICWS versus ^{131}I-mIBG PI for the Curie scoring

A comparison of the Curie scoring of ^{131}I-mBG PICWS and ^{131}I-mIBG PI is summarized in Tables 2 and 3 and Fig. 1c. It was evident that ^{131}I-mIBG PICWS detected more scores than that of ^{131}I-mIBG PI at 39 and that ^{131}I-mIBG PICWS changed the scores of 50% of the studies compared with ^{131}I-mIBG PI. Compared with ^{131}I-mIBG PI, PICWS depicted more scores of each body segment in order of rating in the soft tissues (32 vs. 13) ($n = 10$); the rib, sternum, and scapula (55 vs. 48) ($n = 3$); and the neck and back vertebral column (63 vs. 57) ($n = 2$). Of the 66 images in the series, 12 (18.18%) of the images were concordantly negative with both modalities showing no clinically significant score, 49 (74.24%) of the images were concordantly positive with the two modalities identifying clinically significant scores, and the remaining five (7.58%) images were discordant

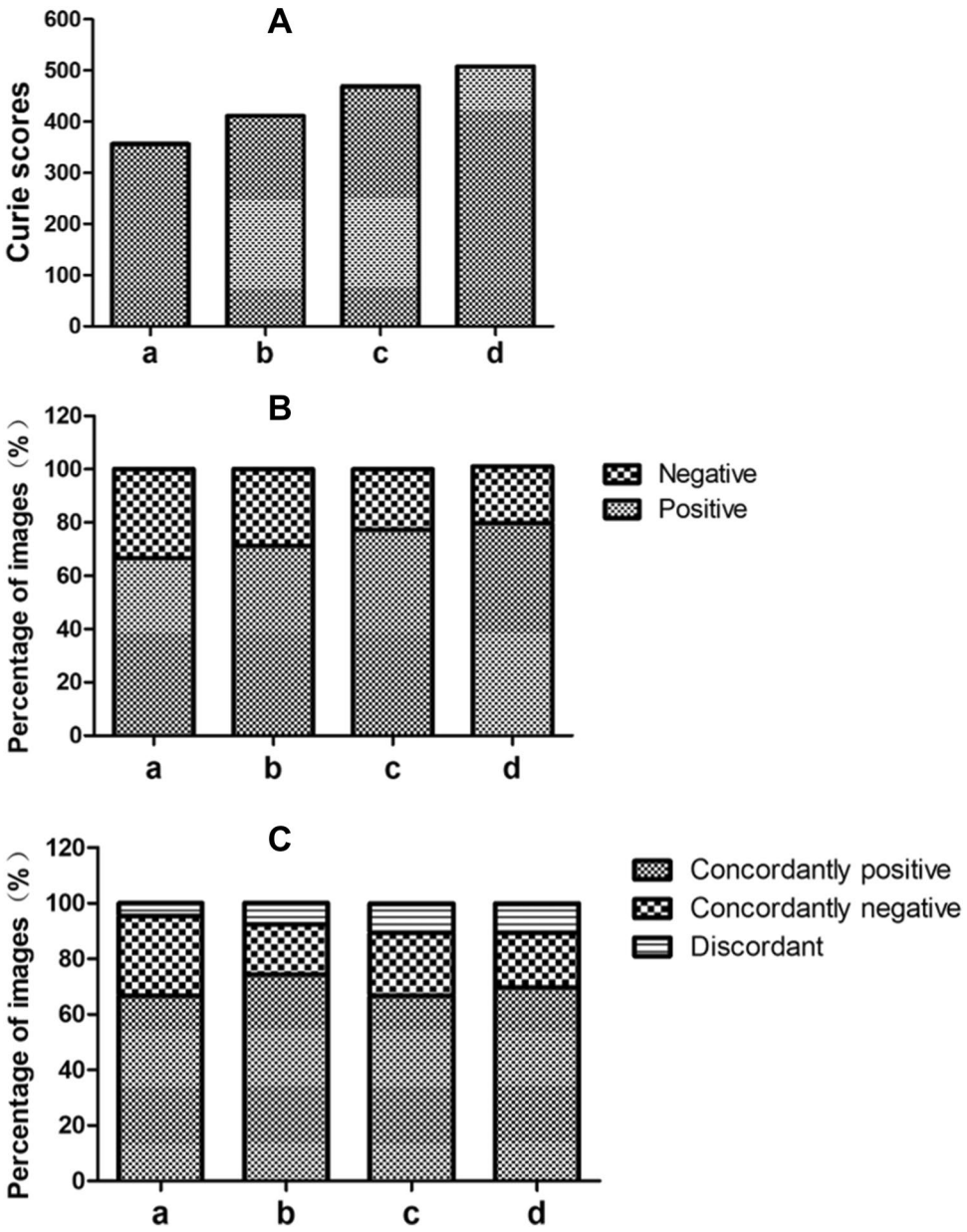

Fig. 1 **a** the Curie scores of the four types of imaging modalities: a, ^{123}I-mIBG PI; b, ^{123}I-mIBG PICWS; c, post-therapeutic ^{131}I-mIBG PI; and d, post-therapeutic ^{131}I-mIBG PICWS. **b** percentage of positive and negative images: a, ^{123}I-mIBG PI; b, ^{123}I-mIBG PICWS; c, post-therapeutic ^{131}I-mIBG PI; and d, post-therapeutic ^{131}I-mIBG PICWS. **c** comparison of the two imaging modalities in the Curie scoring for neuroblastoma: a, ^{123}I-mIBG PICWS versus ^{123}I-mIBG PI; b, ^{131}I-mIBG PICWS versus ^{131}I-mIBG PI; c, ^{123}I- versus ^{131}I-mIBG PI; and d, ^{123}I- versus ^{131}I-mIBG PICWS

with the two modalities displaying different positive or negative results. Of the concordant positive studies, the two modalities had the same scores of 270 in 21 (31.82%) of the images, the remaining 28 (42.42%) with inconsistent scores included findings that ^{131}I-mIBG PICWS was superior to ^{131}I-mIBG PI in 24 (36.36%) of the studies, with total scores of 217 versus 176, and that ^{131}I-mIBG PICWS was inferior to ^{131}I-mIBG PI in 4 (6.06%) of the studies, with total scores of 17 versus 21. Of the disconcordant images, three (4.55%) of the studies with a score of 4 were not detected by ^{131}I-mIBG PI but were detected by ^{131}I-mIBG SPECT/CT, and two (3.03%) of the studies with scores of 2 were seen in ^{131}I-mIBG PI but were confirmed as physiological uptake and contamination by ^{131}I-mIBG SPECT/CT (Fig. 3). The Wilcoxon signed-rank test revealed statistically significant differences in the two modalities ($Z = -3.89$; $P < 0.001$) and showed that PICWS was superior to ^{131}I-mIBG PI in detecting the Curie scores in these studies.

^{123}I- versus ^{131}I-mIBG PI for Curie scoring

A comparison of the Curie scores from ^{123}I-mIBG and ^{131}I-mIBG PI is summarized in Tables 2 and 4 and Fig. 1c. As seen in Table 2, significantly more scores of 113 were noted with ^{131}I-mIBG PI than with ^{123}I-mIBG PI, and 66% (40 of 66) of the studies showed different scores between the two modalities. In terms of each body segment, the top three locations included the lumbar and

Table 3 Comparison of ^{123}I-or ^{131}I-mIBG PICWS vs ^{123}I-or ^{131}I-mIBG PI for Curie scoring in neuroblastoma

PI and PICWS	^{123}I-mIBG PICWS *vs* ^{123}I-mIBG PI		^{131}I-mIBG PICWS vs ^{131}I-mIBG PI	
	No. of image pairs (66)	Scores	No. of image pairs (66)	Scores
Concordantly negative	**19 (28.79%)**	**0**	**12 (18.18%)**	**0**
Concordantly positive	**44 (66.67%)**	**407 vs 356**	**49 (74.24%)**	**504 vs 467**
With same scores in PI and PICWS	14 (21.21%)	125vs 125	21 (31.82%)	270 vs 270
With higher scores in PICWS than in PI	29 (43.94%)	278 vs 226	24 (36.36%)	217 vs176
With lower scores in PICWS than in PI	1 (1.52%)	4 vs 5	4 (6.06%)	17 vs 21
Discordant	3 (4.54%)	4 vs 0	5 (7.58%)	4 vs 2
PI negative and PICWS positive	3 (4.54%)	4 vs 0	3 (4.55%)	4 vs 0
PI positive and PICWS negative	0	0	2 (3.03%)	0 vs 2
PICWS change the scores of PI	**33 (50.00%)**	**286 vs 231**	**33 (50.00%)**	**238 vs 199**

PI planar imaging, *PICWS* planar imaging combined with single-photon emission computed tomography/computed tomography, *mIBG* metaiodobenzylguanidine, *Negative* curie scores for 0, *Positive* curie scores for ≥ 1

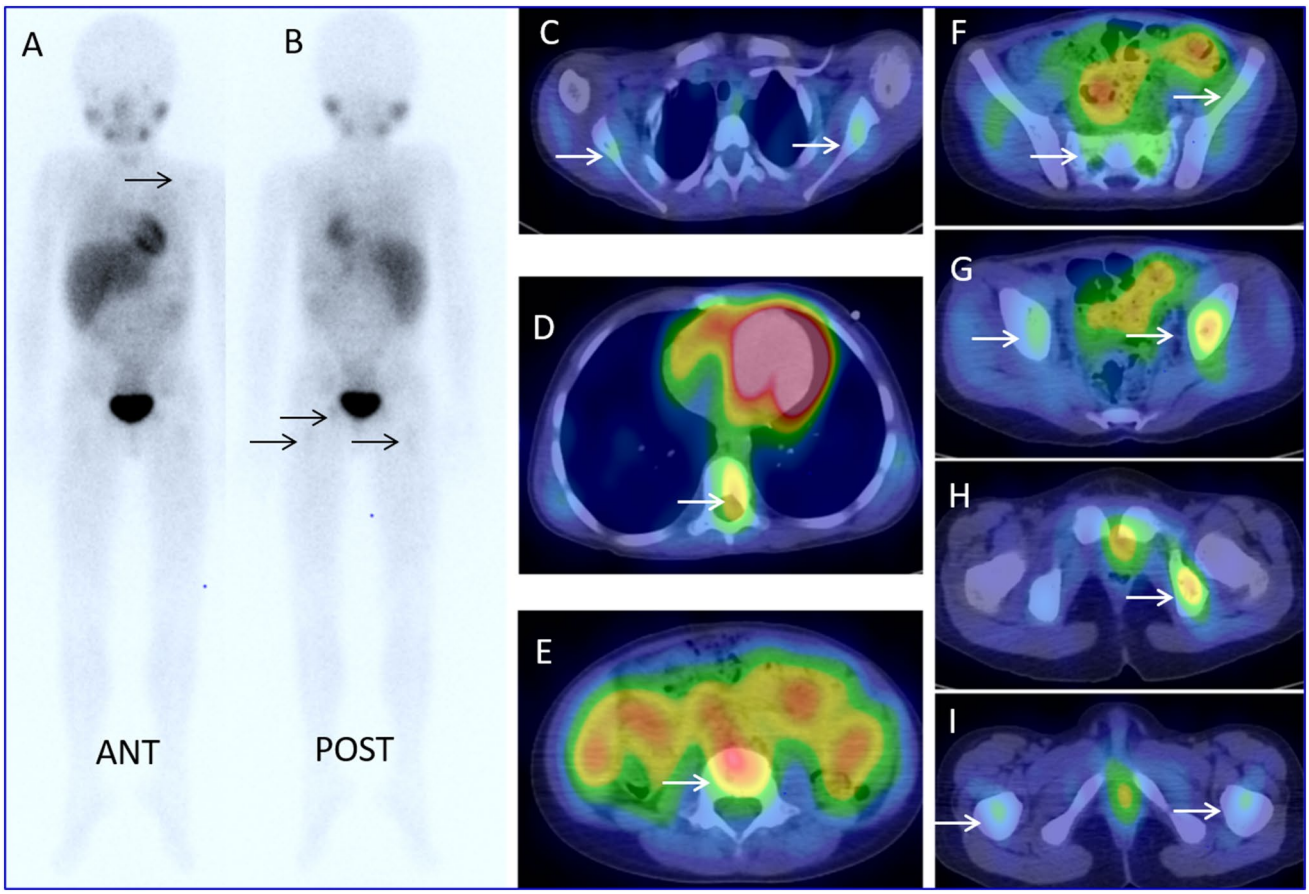

Fig. 2 ^{123}I-mIBG planar and SPECT/CT imaging were conducted in a 7 year-old boy with neuroblastoma within 2 weeks prior to treatment with ^{131}I-mIBG. Curie scores were evaluated for ^{123}I-mIBG planar and SPECT/CT imaging. (**a** and **b**: arrow). In PI, the Curie score was 4 including the ribs, sternum and scapula (3) = 1, the pelvis (5) = 1, and the thighs (8) = 2. In PICWS, the Curie score was 9 including the neck and back vertebral column (2) (**d**, arrow) = 1, the ribs, sternum and scapula (3) (**c**, arrow) = 2, the lumbar and sacral column (4) (**e** and **f**, arrow) = 2, the pelvis (5) (**f**–**h**, arrow) = 2, and the thighs (8) (**i**, arrow) = 2

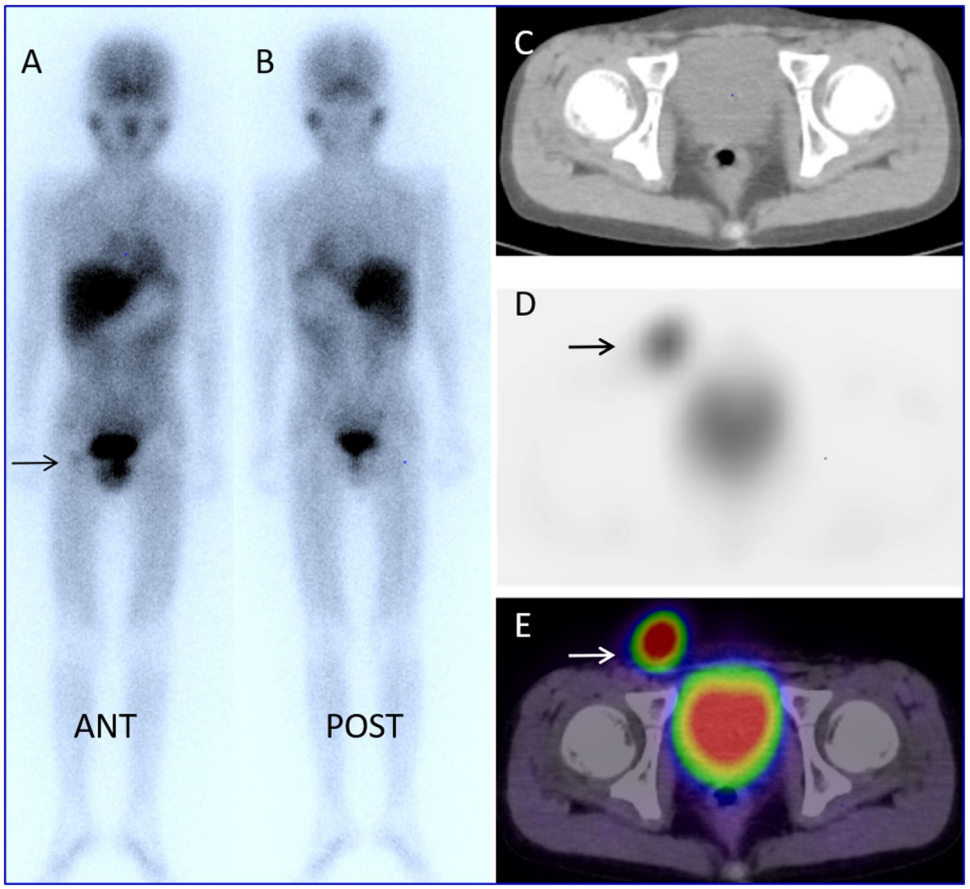

Fig. 3 ^{131}I-mIBG planar and SPECT/CT imaging were conducted in an 8-year-old boy with neuroblastoma 3 days after treatment with ^{131}I-mIBG. Curie scores were evaluated for ^{123}I-mIBG planar and SPECT/CT imaging. In the anterior and posterior view of PI, a lesion (**a** and **b**, arrow) was considered as metastasis in the right pelvis with a score of 1, but it was confirmed as contamination in the PICWS with a score of 0 (**c**–**e**, arrow)

Table 4 Comparison of ^{123}I-*vs* ^{131}I-mIBG imaging for the curie scoring in neuroblastoma

^{123}I- and ^{131}I-mIBG imaging	^{123}I-*vs* ^{131}I-mIBG PI		^{123}I- *vs* ^{131}I-mIBG PICWS	
	No. of image pairs (66)	Scores	No. of image pairs (66)	Scores
Concordantly negative	**15 (22.73%)**	**0**	**13 (19.70%)**	**0**
Concordantly positive	**44 (66.67%)**	**356 vs 456**	**46 (69.70%)**	**409 vs 491**
With same scores in ^{123}I-mIBG and ^{131}I-mIBG imaging	11 (16.67%)	74 vs 74	17 (25.76%)	144 vs 144
With higher scores in ^{123}I-mIBG than ^{131}I-mIBG imaging	1 (1.52%)	9 vs 5	3 (4.55%)	23vs 17
With lower scores in ^{123}I-mIBG than ^{131}I-mIBG imaging	32 (48.48%)	273 vs 377	26 (39.39%)	242 vs 330
Discordant	**7 (10.60%)**	**0 vs 13**	**7 (10.60%)**	**2 vs 17**
^{123}I-mIBG imaging negative and ^{131}I-mIBG imaging positive	7 (10.61%)	0 vs 13	6 (9.09%)	0 vs 17
^{123}I-mIBG imaging positive and ^{131}I-mIBG imaging negative	0	0	1 (1.51%)	2 vs 0
Showing different scores between the two modalities	**40 (60.61%)**	**282 vs 395**	**36 (54.55%)**	**267 vs 364**

mIBG metaiodobenzylguanidine, *PI* planar imaging, *PICWS* planar imaging combined with single-photon emission computed tomography/computed tomography, *Negative* curie scores for 0, *Positive* curie scores for ≥ 1

sacral column (66 vs. 47) ($n = 4$), the pelvis (68 vs. 52) ($n = 5$), and the arms (43 vs. 27) ($n = 6$) visualized with ^{131}I-mIBG PI were significantly higher scores than those visualized with ^{123}I-mIBG PI. In 44 (66.67%) of the 66 studies, there was a concordantly positive score between ^{123}I- and ^{131}I-mIBG PI, with the two modalities showing the same score of 74 in 11 (16.67%) of the images, ^{123}I-mIBG showing lower scores than ^{131}I-mIBG in PI in 32 (48.48%) of the images (273 vs. 377), and ^{123}I-mIBG showing higher scores than ^{131}I-mIBG in PI in 1 (1.52%) image (9 vs. 5). In 15 (22.73%) of the 66 studies, there was a concordantly negative score between ^{123}I- and ^{131}I-mIBG PI, meaning a score of 0. In the seven discordant studies

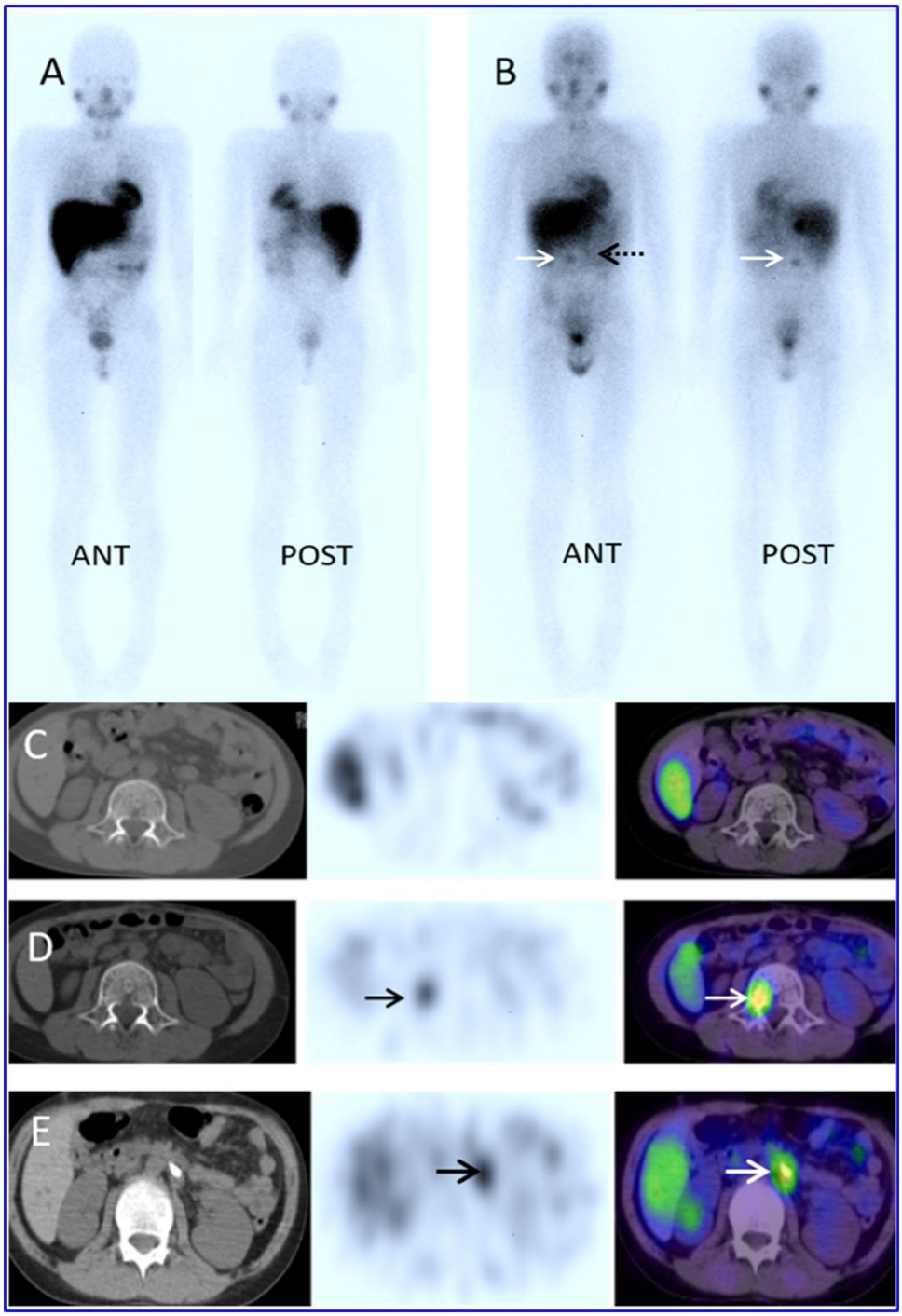

Fig. 4 ^{123}I-mIBG PI and SPECT/CT imaging were conducted 2 weeks prior to ^{131}I-mIBG treatment, and ^{131}I-mIBG PI and SPECT/CT imaging were conducted 4 days after ^{131}I-mIBG treatment, respectively, in an 11 year-old boy with neuroblastoma. ^{123}I-mIBG PI (**a**) and SPECT/CT imaging (**c**) did not show any abnormal mIBG accumulation with a score of 0. In ^{131}I-PI, a lesion was observed in the left upper abdomen region, which was considered as the physiological uptake (**b**, black dotted arrow). A lesion was observed in the lumbar vertebra region, which was considered as the metastases (**b**, white solid arrow) with a score of 1. In PICWS, these two lesions were localized in the lumbar spine (**d**, arrow) and soft tissue (**e**, arrow), respectively, which were considered as the metastases or recurrence with a score of 2

(10.60%), scores were identified by ^{131}I-mIBG but were not detected by ^{123}I-mIBG PI in the seven studies with the scores of 13 (Fig. 4). Although no images were found for which a score could be identified by ^{123}I-mIBG but could not be detected by ^{131}I-mIBG PI, it was observed that there was a statistical difference in the Curie scoring between ^{123}I- and ^{131}I-mIBG PI using the Wilcoxon signed-rank test ($Z = -5.09$; $P < 0.001$).

^{123}I- versus ^{131}I-mIBG PICWS for Curie scoring

A comparison of the Curie scores for ^{123}I- and ^{131}I-mIBG PICWS are shown in Tables 2 and 4 and Fig. 1c. It was noted that ^{131}I-mIBG PICWS exceeded the ability of ^{123}I-mIBG PICWS to detect scores at 97 (508 vs. 411) and 54.55% (36 of 66) of the studies showed different scores between the two modalities. Additionally, we also confirmed that ^{131}I-mIBG PICWS was superior to ^{123}I-mIBG PICWS for Curie scores

in all body segments, with the three segments demonstrating the most obvious advantages in ^{131}I-mIBG PICWS being the thighs ($n=8$) at 16 (66 vs. 50), the neck and back vertebral column ($n=2$) at 16 (63 vs. 47), and the head and face ($n=1$) at 15 (60 vs. 45), respectively. Of the 66 pairs of images, the two imaging modalities showed concordant negative findings in 13 (19.70%) of the studies, showed concordant positive findings in 46 (69.70%) of studies, and showed disconcordant findings in seven (10.60%) of the studies. Among the concordant positive group, ^{131}I-mIBG PICWS with the same scores with ^{123}I-mIBG PICWS were interpreted in 17 (25.76%) studies with scores of 144 vs. 144, ^{131}I-mIBG PICWS with higher scores than those of ^{123}I-mIBG (330 vs. 242) were interpreted in 26 (39.39%) studies, and ^{131}I-mIBG PICWS lower scores than ^{123}I-mIBG PICWS (17 vs. 23) were interpreted in three (4.55%) studies, respectively. There were discordant findings in seven (10.60%) images with 19 scores between ^{123}I- and ^{131}I-mIBG PICWS: six (9.09%) with scores of 17 had positive ^{131}I- and negative ^{123}I-mIBG PICWS (Fig. 4) and one (1.51%) with scores of 2 had negative ^{131}I- and positive ^{123}I-mIBG PICWS. The Wilcoxon signed-rank test showed a statistically significant difference in detecting the Curie scoring between the two modalities ($Z=-5.09$; $P<0.001$).

Discussion

Over the past 20 years, Curie scoring has become an important method for the management of patients with neuroblastomas used by the Children's Oncology Group of North America. Curie scoring divides the skeleton into nine segments, with a tenth added for soft tissue, and scores each segment on a scale of 0–3, resulting in a potential maximum score of 30 [15, 16]. However, most studies have included only ^{123}I- or ^{131}I-mIBG scintigraphy alone to evaluate its diagnostic value for Curie scoring in patients with neuroblastoma [17]. Limited comparative data are available regarding the diagnostic efficacy for Curie scoring with these two modalities. Presently, radionuclide with ^{131}I- and ^{123}I-mIBG routinely includes three scanning modalities: diagnostic ^{123}I-mIBG scintigraphy, diagnostic ^{131}I-mIBG scintigraphy, and post-therapeutic ^{131}I-mIBG scintigraphy. At our institute, ^{123}I-mIBG scintigraphy was usually conducted for patients with neuroblastoma prior to ^{131}I-mIBG treatment to indicate the ^{131}I-mIBG therapy according to the results of scintigraphy, because the image quality of ^{123}I-mIBG scintigraphy is generally superior to diagnostic ^{131}I-mIBG scintigraphy [18, 19], which was not examined in our department. After ^{131}I-mIBG therapy, it is recommended that ^{131}I-mIBG imaging be used to confirm the mIBG accumulation in lesions. In the present study, we compared the diagnostic value between the ^{123}I-mIBG scintigraphy and post-therapeutic ^{131}I-mIBG scintigraphy for evaluating the Curie scoring in these patients with neuroblastoma. Furthermore, precise localization of the foci of ^{123}I- or ^{131}I-mIBG uptake is sometimes formidable as a result of the lack of anatomic landmarks in PI, and physiological uptake is not always easily differentiable from pathological uptake, which seriously affects the results of Curie scoring. Integrated SPECT/CT can provide both metabolic and anatomic information regarding a lesion. An improvement in diagnostic accuracy for ^{123}I- or ^{131}I-mIBG PI has been shown using SPECT/CT in various neuroendocrine tumors [20–22]. The present study also aimed to evaluate the diagnostic performance of ^{123}I- and post-therapeutic ^{131}I-mIBG PICWS compared with PI for Curie scoring in patients with neuroblastoma.

In the present study, we found that ^{123}I- or ^{131}I-mIBG PICWS could detect more scores than that of ^{123}I- or ^{131}I-mIBG PI according to the criteria of Curie scoring. Additionally, we also confirmed that both ^{123}I- and ^{131}I-mIBG PICWS could provide the change of scores in 50% of studies compared with ^{123}I- and ^{131}I-mIBG PI, respectively, in these 66 pairs of imaging of 62 patients with neuroblastoma. A comparison of the results between ^{123}I-PI and ^{123}I-mIBG PICWS and between ^{131}I-PI and ^{131}I-mIBG PICWS for Curie scoring in neuroblastoma are shown in Tables 2 and 3, respectively. Many studies have demonstrated the incremental value of SPECT/CT compared with PI in various neuroendocrine tumors. For example, in differentiated thyroid cancer, Spanu et al. reported that ^{131}I-PICWS had an added value compared with PI in 67.8% of patients, improved therapeutic management in 35.6% of positive patients, and avoided unnecessary ^{131}I treatment in 20.3% of patients with physiological uptake or only a single benign lesion [23]. In patients with malignant pheochromocytoma or paraganglioma and neuroblastoma, Fukuoka et al. found that unknown lesions in ^{123}I-mIBG PI could be identified using ^{123}I-mIBG SPECT/CT in 45.2% of images from 68.8% of patients and that anatomic locations of the lesions were modified by SPECT/CT imaging in 45.2% of images from 62.5% of patients. Unknown lesions in post-therapeutic ^{131}I-mIBG PI could be seen by SPECT/CT in 23.5% of studies in 33.3% of the patients and anatomic locations of the lesions were altered by SPECT/CT in 47.1% of studies in 66.7% of patients [9]. In patients with neuroblastoma, Theerakulpisut et al. demonstrated that ^{131}I-mIBG SPECT/CT found additional lesions in 23.2% of the cases, assisted localization of lesions in 21.1% of the cases, resolved questionable findings in 85.7% of the cases, determined the functional status of lesions in anatomical imaging in 94.4% of the cases, and changed from negative to positive diagnosis in 19.5% of the cases [24]. For Curie scoring, Černý et al. confirmed that, compared with ^{123}I-mIBG PI, ^{123}I-mIBG PICWS could detect additional scores in 54% of the patients,

which was basically consistent with our study, and SPECT/CT scintigraphy was recommended to conduct evaluation Curie scoring in neuroblastoma, particularly for patients with clinical III and IV stages [25]. Additionally, Černý et al. [25] and Theerakulpisut et al. [24] also found that the most common site of added detection by PICWS compared with PI was the intra-abdominal lymph node metastases of neuroblastoma. In the present study, the body segment with the most added detection of ^{123}I or ^{131}I-mIBG PICWS compared with PI were soft tissue lesions, which suggests consistency with the two abovementioned studies [24, 25].

It is well known that ^{123}I-mIBG is significantly superior to ^{131}I-mIBG in terms of diagnostic imaging, making it the agent of choice for scintigraphy of pediatric neuroblastoma [7, 8]. For Curie scores, it was reported by Naranjo et al. that there were no differences in median Curie scores between diagnostic ^{123}I- and ^{131}I-mIBG PI at any time-point, including diagnosis, post-induction, post-transplant, and post-biotherapy [26]. By contrast, ^{131}I-mIBG scintigraphy has clear advantages compared with ^{123}I-mIBG scintigraphy, including ^{131}I- versus ^{123}I-mIBG PI and ^{131}I- versus ^{123}I-mIBG PICWS, in detecting Curie scores in patients with neuroblastoma in the current study. There may be three main possible reasons for this difference. First, Shapiro et al. [27] reported that it is possible to use doses of ^{123}I-mIBG 20 times as large as doses of ^{131}I-mIBG with equivalent absorbed radiation doses because of the characteristics of ^{123}I and ^{131}I, which means that the doses of ^{123}I-mIBG using 111 and 222 MBq for scintigraphy imaging was equivalent to almost 2.22 and 4.44 Gbq (60 mCi and 120 mCi), respectively, of ^{131}I in image quality in patients with neuroblastoma. Therefore, the doses of diagnostic ^{123}I-mIBG were obviously less than the therapeutic dose of ^{131}I-mIBG (mean, 417 mCi in the present study) for image quality. Secondly, the Japanese Ministry of Health, Labor and Welfare recommend that ^{123}I-mIBG scintigraphy was usually conducted at 24 h after injection, and additional images were available at 6 or 48 h after administration if required. In our study, ^{123}I-mIBG PI was usually conducted at 6 and 24 h and after injection, and SPECT/CT was conducted following the ^{123}I-mIBG PI at 6 h. Therefore, the scanning time of 6 h may be too short to affect image quality. Our previous studies have also shown that 24 h images with ^{123}I-mIBG could detect more lesions than the 6 h images with ^{123}I-mIBG in 53% (8 of 15) of patients with malignant pheochromocytoma and paraganglioma [28]. Furthermore, the ^{123}I-mIBG scanning speed was faster than that recommended by the European Association of Nuclear Medicine guidelines [14] (15 vs. 5 cm/min), which may also affect image quality.

Although ^{123}I-or ^{131}I-mIBG scintigraphy has been recognized as the main imaging procedure for diagnosis, staging, and response assessment of neuroblastoma, false-negative mIBG scintigraphy leading to the incorrect diagnosis and staging of the disease were found in approximately 8% of patients with neuroblastoma [29]. Recently, a few positron emission tomography (PET) tracers have been tested as effective substitutes for ^{123}I- or ^{131}I-mIBG in assessing neuroblastoma such as ^{18}F-FDG[30], ^{68} Ga-DOTATATE [31], ^{18}F-DOPA [32, 33], labeled monoclonal antibody [34], and ^{124}I-mIBG[35]. For example, ^{18}F-DOPA PET/CT has already been proven to be more sensitive than ^{123}I-mIBG scintigraphy for detecting the recurrence of neuroblastoma [33]. Specifically, it has been shown to be a reliable diagnostic procedure for detecting small soft tissue and bone metastases that could not be accurately detected with ^{123}I-mIBG scintigraphy [32, 33]. However, despite these techniques being available for the imaging of neuroblastoma, the high cost and the availability of PET tracers limits their application. Furthermore, most of these studies with a small sample size and retrospective nature also need further research. Therefore, ^{123}I- or ^{131}I-mIBG scanning remains the gold standard for the evaluation of neuroblastoma.

The present study has several limitations that must be acknowledged. First, it has certain inherent limitations associated with its retrospective design. Second, we only registered patients from a single tertiary referral center, and we included a relatively limited number of patients. Third, because of the modality of different therapies conducted before or after ^{131}I-mIBG treatment, we did not evaluate the correlation between the Curie scores and prognosis in these patients with neuroblastoma. Fourth, a few patients were subjected to an injecting dose of 111 MBq for ^{123}I-mBIG scintigraphy before May 2011, which may affect its ability to detect metastatic or recurrent disease in patients with neuroblastoma. Furthermore, SPECT/CT was not conducted after ^{123}I-mIBG PI at 24 h; so, these images were not included in the comparative study.

Research has demonstrated that Curie scoring has been developed to predict the treatment response and prognosis of the mIBG-avid disease in neuroblastoma [15, 16]. For example, using this method, Yanik et al.[17] confirmed that Curie scoring has importantly prognostic value in the management of patients with high-risk neuroblastoma. In particular, patients with Curie scores ≥ 2 after induction chemotherapy have extremely poor outcomes and alternative treatment strategies should be considered [15, 16]. However, we did not evaluate the correlation between the Curie scores and prognosis in these patients with neuroblastoma in the present study. In the future, comparing the diagnostic value between ^{123}I-mIBG and ^{131}I-mIBG scan, including PI and PICWS for the Curie scoring in evaluating the treatment response and prognosis of neuroblastoma, may have useful clinical research perspectives.

Conclusion

In conclusion, the present study demonstrates that post-therapy ^{131}I-mIBG scintigraphy is superior to diagnostic ^{123}I-mIBG scintigraphy for the evaluation of Curie scoring in patients with neuroblastoma, including ^{131}I- vs. ^{123}I-mIBG PI and ^{131}I- vs. ^{123}I-mIBG PICWS. We also confirmed that ^{131}I- and ^{123}I-mIBG PICWS are more helpful in the evaluation of Curie scores than PI, especially in the evaluation of Curie scoring for soft tissue lesions.

Author contributions DK and SK designed the present study. ZLQ and SS conducted the statistical analysis. ZLQ and SS collected the clinical data. ZLQ wrote the whole paper. ZLQ, DK, and HW supervised and edited the paper. All authors read and approved the final paper.

Compliance with ethical standards

Conflict of interest The authors declare that they have no conflict of interest.

Ethical approval The study protocol was approved by the Ethics Committee of the Kanazawa University Hospital.

References

1. Matthay KK, Villablanca JG, Seeger RC, Harris RE, Ramsay NK, et al. Treatment of high-risk neuroblastoma with intensive chemotherapy, radiotherapy, autologous bone marrow transplantation, and 13-cis-retinoic acid. Children's Cancer Group. N Engl J Med. 1999;341:1165–73.
2. Heck JE, Ritz B, Hung RJ, Hashibe M, Boffetta P. The epidemiology of neuroblastoma: a review. Paediatr Perinat Epidemiol. 2009;23:125–43.
3. Moroz V, Machin D, Faldum A, Hero B, Iehara T, Mosseri V, et al. Changes over three decades in outcome and the prognostic influence of age-at-diagnosis in young patients with neuroblastoma: a report from the International Neuroblastoma Risk Group Project. Eur J Cancer. 2011;47:561–71.
4. Parisi MT, Eslamy H, Park JR, Shulkin BL, Yanik GA. 131I-Metaiodobenzylguanidine theranostics in neuroblastoma: historical perspectives. Practical applications. Semin Nucl Med. 2016;46:184–202.
5. Cohn SL, Pearson AD, London WB, Monclair T, Ambros PE, Brodeur GM, et al. The international neuroblastoma risk group (INRG) classification system: an INRG task force report. J Clin Oncol. 2009;27:289–97.
6. Radovic B, Artiko V, Sobic-Saranovic D, Trajkovic G, Markovic S, Vujic D, et al. Evaluation of the SIOPEN semi-quantitative scoring system in planar simpatico-adrenal MIBG scintigraphy in children with neuroblastoma. Neoplasma. 2015;62:449–55.
7. Furuta N, Kiyota H, Yoshigoe F, Hasegawa N, Ohishi Y. Diagnosis of pheochromocytoma using [123I]-compared with [131I]-metaiodobenzylguanidine scintigraphy. Int J Urol. 1999;6:119–24.
8. Koopmans KP, Neels ON, Kema IP, Elsinga PH, Links TP, de Vries EGE, et al. Molecular imaging in neuroendocrine tumors: molecular uptake mechanisms and clinical results. Crit Rev Oncol Hematol. 2009;71:199–213.
9. Fukuoka M, Taki J, Mochizuki T, Kinuya S. Comparison of diagnostic value of I-123 MIBG and high-dose I-131 MIBG scintigraphy including incremental value of SPECT/CT over planar image in patients with malignant pheochromocytoma/paraganglioma and neuroblastoma. Clin Nucl Med. 2011;36:1–7.
10. Wong KK, Gandhi A, Viglianti BL, Fig LM, Rubello D, Gross MD. Endocrine radionuclide scintigraphy with fusion single photon emission computed tomography/computed tomography. World J Radiol. 2016;8:635–55.
11. Scherübl H, Raue F, Frank-Raue K. Neuroendocrine tumors : Classification, clinical presentation and imaging. Radiologe. 2019;59:952–60.
12. Riaz S, Bashir H, Khan SJ, Qazi A. I-131 mIBG scintigraphy curie versus SIOPEN scoring: prognostic value in stage 4 neuroblastoma. Mol Imaging Radionucl Ther. 2018;27:121–5.
13. Decarolis B, Schneider C, Hero B, Simon T, Volland R, Roels F, et al. Iodine-123 metaiodobenzylguanidine scintigraphy scoring allows prediction of outcome in patients with stage 4 neuroblastoma: results of the Cologne interscore comparison study. J Clin Oncol. 2013;31:944–51.
14. Olivier P, Colarinha P, Fettich J, Fischer S, Frökier J, Giammarile F, et al. Guidelines for radioiodinated MIBG scintigraphy in children. Eur J Nucl Med Mol Imaging. 2003;30:B45-50.
15. Matthay KK, Edeline V, Lumbroso J, Tanguy ML, Asselain B, Zucker JM, et al. Correlation of early metastatic response by 123I-metaiodobenzylguanidine scintigraphy with overall response and event-free survival in stage IV neuroblastoma. J Clin Oncol. 2003;21:2486–91.
16. Messina JA, Cheng SC, Franc BL, Charron M, Barry Shulkin B, To B, et al. Evaluation of semi-quantitative scoring system for metaiodobenzylguanidine (mIBG) scans in patients with relapsed neuroblastoma. Pediatr Blood Cancer. 2006;47:865–74.
17. Yanik GA, Parisi MT, Shulkin BL, Naranjo A, Kreissman SG, London WB, et al. Semiquantitative mIBG scoring as a prognostic indicator in patients with stage 4 neuroblastoma: a report from the Children's oncology group. J Nucl Med. 2013;54:541–8.
18. Lynn MD, Shapiro B, Sisson JC, Beierwaltes WH, Meyers LJ, Ackerman R, et al. Pheochromocytoma and the normal adrenal medulla: improved visualization with I-123 MIBG scintigraphy. Radiology. 1985;155:789–92.
19. Shulkin BL, Shapiro B, Francis IR, Dorr R, Shen SW, Sisson JC. Primary extra-adrenal pheochromocytoma: positive I-123 MIBG imaging with negative I-131 MIBG imaging. Clin Nucl Med. 1986;11:851–4.
20. Pfannenberg AC, Eschmann SM, Horger M, Lamberts R, Vonthein R, Claussen CD, et al. Benefit of anatomical-functional image fusion in the diagnostic work-up of neuroendocrine neoplasms. Eur J Nucl Med Mol Imaging. 2003;30:835–43.
21. Moreira AP, Duarte LH, Vieira F, João F, Lima JP. Value of SPET/CT image fusion in the assessment of neuroendocrine tumours with 111In-pentetreotide scintigraphy. Rev Esp Med Nucl. 2005;24:14–8.
22. Rozovsky K, Koplewitz BZ, Krausz Y, Revel-Vilk S, Weintraub M, Chisin R, et al. Added value of SPECT/CT for correlation of MIBG scintigraphy and diagnostic CT in neuroblastoma and pheochromocytoma. AJR Am J Roentgenol. 2008;190:1085–90.
23. Spanu A, Solinas ME, Chessa F, Sanna D, Nuvoli S, Madeddu G. 131I SPECT/CT in the follow-up of differentiated thyroid carcinoma: incremental value versus planar imaging. J Nucl Med. 2009;50:184–90.
24. Theerakulpisut D, Raruenrom Y, Wongsurawat N, Somboonporn C. Value of SPECT/CT in diagnostic I-131 MIBG scintigraphy in patients with neuroblastoma. Nucl Med Mol Imaging. 2018;52:350–8.

25. Černý I, Prášek J, Kašpárková H. Superiority of SPECT/CT over planar 123I-mIBG images in neuroblastoma patients with impact on Curie and SIOPEN score values. Nuklearmedizin. 2016;55:151–7.
26. Naranjo A, Parisi MT, Shulkin BL, London WB, Matthay KK, Kreissman SG, et al. Comparison of ^{123}I-metaiodobenzylguanidine (MIBG) and ^{131}I-MIBG semi-quantitative scores in predicting survival in patients with stage 4 neuroblastoma: a report from the Children's Oncology Group. Pediatr Blood Cancer. 2011;56:1041–5.
27. Shapiro B, Gross MD. Radiochemistry, biochemistry, and kinetics of 131I-metaiodobenzylguanidine (MIBG) and 123I-MIBG: clinical implications of the use of 123I-MIBG. Med Pediatr Oncol. 1987;15:170–7.
28. Kayano D, Taki J, Fukuoka M, Wakabayashi H, Inaki A, Nakamura A, et al. Low-dose (123)I-metaiodobenzylguanidine diagnostic scan is inferior to (131)I-metaiodobenzylguanidine post-treatment scan in detection of malignant pheochromocytoma and paraganglioma. Nucl Med Commun. 2011;32:941–6.
29. Biasotti S, Garaventa A, Villavecchia GP, Cabria M, Nantron M, De Bernardi B. False-negative metaiodobenzylguanidine scintigraphy at diagnosis of neuroblastoma. Med Pediatr Oncol. 2000;35(2):153–5.
30. Bleeker G, Tytgat GA, Adam JA, Caron HN, Kremer LCM, Hooft L, et al. 123I-MIBG scintigraphy and 18F-FDG-PET imaging for diagnosing neuroblastoma. Cochrane Database Syst Rev. 2015;1:009263.
31. Kong G, Hofman MS, Murray WK, Wilson S, Wood P, Downie P, et al. Initial experience with gallium-68 DOTA-octreotate PET/CT and Peptide Receptor Radionuclide Therapy For Pediatric Patients With Refractory Metastatic Neuroblastoma. J Pediatr Hematol Oncol. 2016;38(2):87–96.
32. Piccardo A, Lopci E, Conte M, Garaventa A, Foppiani L, Altrinetti V, et al. Comparison of 18F-dopa PET/CT and 123I-MIBG scintigraphy in stage 3 and 4 neuroblastoma: a pilot study. Eur J Nucl Med Mol Imaging. 2012;39:57–71.
33. Piccardo A, Puntoni M, Lopci E, Conte M, Foppiani L, Sorrentino S, et al. Prognostic value of ^{18}F-DOPA PET/CT at the time of recurrence in patients affected by neuroblastoma. Eur J Nucl Med Mol Imaging. 2014;41:1046–56.
34. Reuland P, Geiger L, Thelen MH, Handgretinger R, Haase B, Müller-Schauenburg W, et al. Follow-up in neuroblastoma: comparison of metaiodobenzylguanidine and a chimeric anti-GD2 antibody for detection of tumor relapse and therapy response. J Pediatr Hematol Oncol. 2001;23:437–42.
35. Cistaro A, Quartuccio N, Caobelli F, Piccardo A, Paratore R, Coppolino P, et al. 124I-MIBG: a new promising positron-emitting radiopharmaceutical for the evaluation of neuroblastoma. Nucl Med Rev Cent East Eur. 2015;18:102–6.